Proc. of the 9th International Symposium on Geotechnical Safety and Risk (ISGSR)
Edited by Zhongqiang Liu, Jian Dai and Kate Robinson
Published by Research Publishing, Singapore.
doi: 10.3850/GRF-25280825_isgsr-028-P096-cd

ISGSR2025

Reliability Analysis of 3D Railway Embankment Considering Anisotropic Soil Spatial Variability and Train Load Distribution

Wei Huang, Michael A. Hicks

Department of Geoscience and Engineering, Delft University of Technology, Delft, The Netherlands.
E-mail: W.Huang-1@tudelft.nl, M.A.Hicks@tudelft.nl

Abstract: The Random Finite Element Method has been used to investigate the influence of anisotropic spatial variability of soil shear strength on the failure probability and consequence of an idealized three-dimensional (3D) slope subjected to different lengths of static surcharge loads, to give a simplified representation of a railway embankment subjected to train loading. For each studied case, the probability of design failure has been computed as a function of the factor of safety (*FoS*) based on 500 realizations. The results demonstrate the combined effect of the spatial correlation of soil strength and the load distribution along the slope length on the probabilistic characteristics of the system response.

Keywords: railway embankment, Random Finite Element Method, reliability analysis, soil spatial variability, three-dimensional random field, train load.

1. Introduction

Railway embankment stability is dependent on the embankment geometry, the ground conditions, and the train load characteristics. Many assumptions exist in a conventional deterministic design and assessment framework, including plane strain conditions, homogeneous soil layers, and uniformly distributed infinite line loads (Bogusz & Godlewski, 2019). However, these simplifications tend to yield over-conservative designs and assessments by neglecting 3D soil heterogeneity (Lodahl et al., 2012) and load distributions (Savolainen et al., 2017).

The Random Finite Element Method (RFEM) is a well-established stochastic approach for tackling the complexity of intrinsic soil spatial variability and its influence on geotechnical systems (Griffiths & Fenton, 2000). Among the considerable amount of geotechnical research conducted using RFEM, the work here is based on previous findings on the influence of anisotropic soil heterogeneity on 2D (Hicks & Samy, 2002) and 3D (Hicks & Spencer, 2010; Hicks et al., 2014; Li et al., 2015; Varkey et al., 2023) slope reliability, and on the in-house code developed by these authors. The key addition here is the application of surface loads on the crest of the slope, which requires slope reliability to be determined as a function of ultimate bearing capacity. The simplified railway embankment is analogous to the classical 'footing-on-slope' problem (Meyerhof, 1957; Azzouz & Baligh, 1983).

2. Problem Definition and Methodology

2.1. *Problem description*

Figure 1 shows the idealized slope geometry. A uniform vertical surcharge, with a width of 3 m (x-direction) and a length L_q (y-direction), resembling a flexible rectangular surface footing, is located at a distance of 2 m from the slope crest. The domain is discretized by 11800, 20-node, brick elements of size 1.0×1.0×1.0 m except along the slope face, and a reduced integration scheme of 2×2×2 Gauss points per element. The boundary conditions comprise a fully restrained base, 2D rollers on the two vertical y-z faces preventing movement in the x direction, and 1D rollers on the two end (x-z) faces allowing movement only in the z-direction (Hicks et al., 2014).

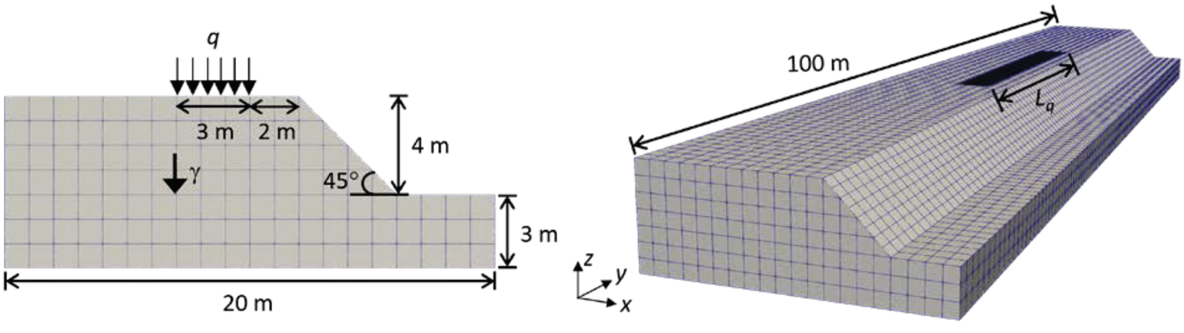

Figure 1. Problem geometry and finite element mesh: 2D view (left) and 3D view (right).

A single soil type under undrained conditions is considered, for which an elastic-perfectly plastic Tresca soil model is adopted with the (mean) parameter values listed in Table 1. The undrained bearing capacity q_u

of the specific ‘footing-on-slope’system is computed by incrementally increasing the load until failure, as indicated by non-convergence after 500 equilibrium iterations. A dimensionless bearing capacity factor, $N_c = q_u/c_u$, can then be back-calculated to facilitate further (probabilistic) analysis (e.g., Georgiadis, 2010; Luo & Bathurst, 2017).

Table 1. Soil parameter (mean) values.

Unit weight: γ	Undrained shear strength: c_u	Young’s modulus: E	Poisson’s ratio: ν
20 [kN/m^3]	20 [kPa]	3×10^4 [kPa]	0.3 [-]

2.2. *Probabilistic analysis using RFEM*

For simplicity, only undrained shear strength c_u is treated as spatially variable. Random fields (RFs) of c_u have been generated using Local Average Subdivision (LAS) based on an exponential Markov covariance function (Fenton & Vanmarcke, 1990). This requires the point and spatial statistics of c_u as input: i.e., mean μ_c and standard deviation σ_c, which combine to give the coefficient of variation $COV_c = \sigma_c/\mu_c$; and Cartesian scales of fluctuation, i.e., θ_x, θ_y, θ_z. For anisotropic RFs, the method here is to squash and/or stretch isotropic RFs to achieve the required anisotropy level (Hicks & Spencer, 2010). A normal distribution of c_u, truncated to avoid negative values, is assumed, as is reasonable for COV_c = 0.2 (Hicks & Samy, 2002). As the focus is on the influence of soil variability in the y-direction for various load lengths, θ and θ have fixed values while different combinations of θ_y and L_q have been studied (Table 2). A 2D (plane strain) case is used as a stochastic baseline, which implies θ_y=L_q = inf.

Table 2. Input statistics of c_u and values of L_q for different cases investigated by RFEM.

	2D (plane strain)	3D				
θ_y[m]	•	16	16	16	30	60
L_q[m]	•	100	60	30	30	30
Fixed parameters	μ_c = 20 [kPa], COV_c = 0.2 [-], θ_x =16 [m], θ_z = 2 [m]					

The RFs are mapped to the FE mesh at the Gauss point level. Each RFEM analysiscomprises 500 realizations, which prove to be sufficient for statistical convergence of the output N_c, enabling meaningful probabilistic interpretation of the results for N_c and quantities measuring failure consequence, i.e., failure volume and length, which are derived from the failed mass identified by a K-means clustering algorithm (Huang et al., 2013; van den Eijnden & Hicks, 2017). The probability of design failure (P_f) linking realized N_c values to the deterministic design value is calculated as (Griffiths & Fenton, 2001; Luo & Bathurst, 2017)

$$P_f = P(N_c < N_{c,det}/FoS) \approx \sum_{i=1}^{n} I(N_{c,i} < N_{c,det}/FoS)\Big/n \tag{1}$$

where $N_{c,\,i} = q_{u\,,i}/\mu_c$ is obtained from the i-th realization, n is the total number of realizations, and $I(\bullet)$ is a Boolean function equal to 1 if its argument is true or 0 otherwise; $N_{c,det}$ is the deterministic solution given by a conventional (plane strain) analysis, and this is factored down by a given FoS to serve as the design value.

3. Results and Discussion

Figure 2 shows the histogram of N_c for each RFEM analysis, as well as failure volumes/lengths expressed as a percentage of the total mesh volume/length. Note that failure lengths in 2D are implicitly infinite and therefore not plotted in Figure 2(a). The deterministic N_c obtained for a homogeneous slope with c_u=μ_c is also plotted, on which associated failure volume and length are superimposed in bold black markers.

Figures 2(a) and (b) indicate a significant difference between 2D and 3D stochastic analyses for the same θ_x and θ_z, and the slope loaded along its entire length. The distribution of N_c has a much narrower range and a lower mean value in the 3D case, as well as a wide range of possible failure lengths and a more concentrated distribution of failure volumes. The relatively small value of θ_y (relative to slope length) allows 3D failure to seek a ‘favorable’ path through semi-continuous weaker zones. In contrast, the average failure volume in 2D or from the deterministic analysis is overestimated because a whole-length failure is ‘enforced’ by the underlying assumptions.

Such observations do not apply to 3D cases in which L_q is much smaller than the slope length and $L_q/2 \le \theta_y \le 2L_q$, as in Figures 2(d)-(f). In these plots, the deterministic failure length and volume appear to be a fair representation of the average stochastic response, even though the failure length distribution is somewhat wider for smaller θ_y. The smaller L_q seems to dominate slope responses for different θ_y in the three scenarios, leading to similar statistics of N_c and failure volume, and average failure lengths around the same as L_q (=30 m).

The influential role of L_q is highlighted in Figures 2(b)-(d) from another perspective when θ_y is constant and relatively small. As L_q gets larger, from around 1/3 of the slope length up to the slope length, the deterministic solution increasingly overestimates the mean stochastic response. A longer load means a greater region under its influence; hence, potential failures can follow a greater variety of paths due to the spatial variability, promoting shorter and more localized failures while making failure more likely under a smaller load. Note that the (unfactored) deterministic bearing capacity of the slope is non-conservative in all cases analyzed.

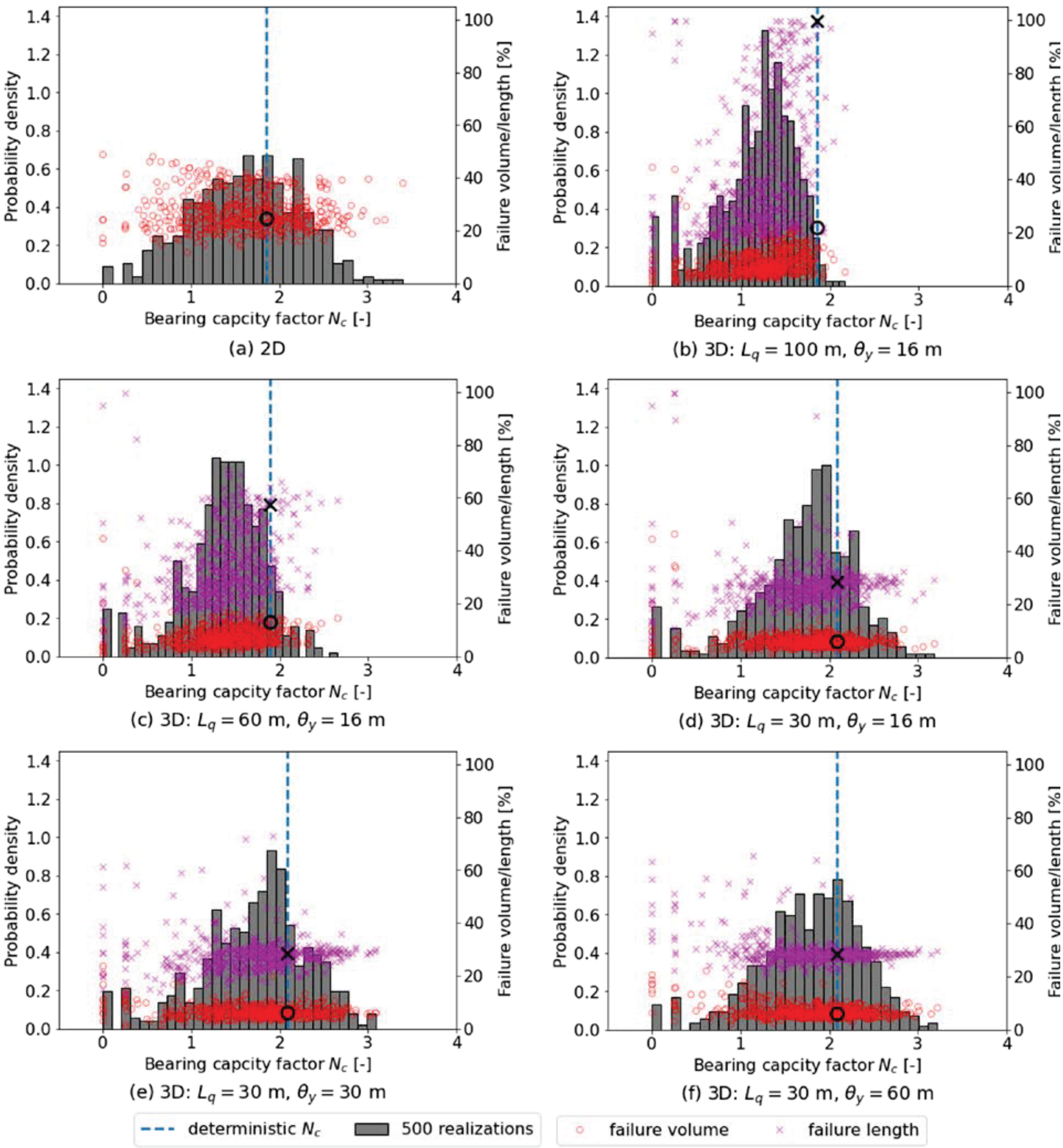

Figure 2. Probability density functions of N_c and failure volumes and lengths for different cases obtained by RFEM.

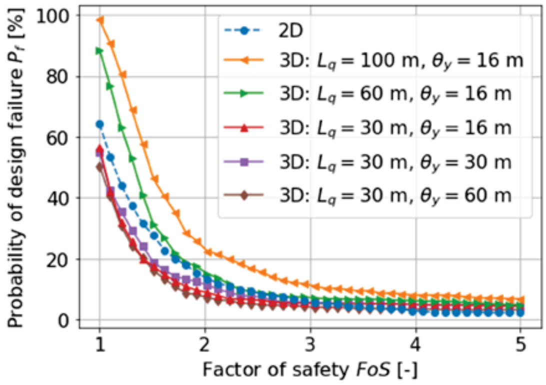

Figure 3. Probability of design failure vs. factor of safety for different cases investigated by RFEM.

Figure 3 presents the connection between P_f calculated according to Eq. (1) and a range of FoS values that might be adopted in 2D deterministic design for the RFEM-investigated cases. It shows consistent observations as before, including: 1) a significant difference between the 2D case and the 3D plane-strain-equivalent case with θ_y=16 m, with the former overestimating the system reliability throughout the plotted range (i.e., lower P_f for a given FoS); 2) higher P_f for larger L_q when fixing θ_y, as the overall load bearing capacity is lower (i.e., distribution of N_c shifted to the left), especially for FoS<3; 3) negligible differences among the three cases of L_q=30 m with varied θ_y. Furthermore, the 2D reliability analysis is only conservative for cases where $L_q\,/\theta_y < 2$. Naturally, a higher FoS gives a more reliable design, but to ensure a desirable level of system reliability (e.g., P_f <5%), a one-fit-all FoS for the embankment under different soil heterogeneity and loading scenarios can only be asymptotically obtained by FoS > 5, which might not be acceptable in practice. Hence, tailored probabilistic analysis taking into account the heterogeneous ground conditions and realistic load distributions is vital to arrive at economical and safe designs.

4. Conclusions

Full probabilistic analyses using RFEM have highlighted the need for 3D reliability analysis of loaded heterogeneous slopes, e.g., railway embankments, under certain circumstances. The bearing capacity of these embankments is of paramount importance for reliable performance in service, which has been shown to depend on not only the load distribution but also the spatial variability of soil strength. The results have demonstrated the decisive role of the ratio between the load length (L_q) and the longitudinal scale of fluctuation (θ_y) of soil heterogeneity in reliability-based assessments. 2D reliability analysis is sufficient only when $L_q/\theta_y < 2$ or a cautiously large FoS is to be applied without prior knowledge of L_q or θ_y. If the failure-related risk is to be evaluated, 3D stochastic modeling can be necessary to quantify failure consequences, such as probabilistic distributions of failure length and volume.

Acknowledgements

This work is part of the research program RESET ("Rail Embankments for the Safe Expansion of rail Traffic") funded by ProRail, and has used the Dutch national e-infrastructure with the support of the SURF Cooperative using grant no. EINF-8424. The authors also acknowledge the use of computational resources of the DelftBlue supercomputer, provided by Delft High Performance Computing Centre (https://www.tudelft.nl/dhpc).

References

Azzouz, A. S., & Baligh, M. M. (1983). Loaded areas on cohesive slopes. *Journal of Geotechnical Engineering*, *109*(5), 724–729. Scopus. https://doi.org/10.1061/(ASCE)0733-9410(1983)109:5(724)

Bogusz, W., & Godlewski, T. (2019). Geotechnical design of railway embankments – requirements and challenges. *MATEC Web of Conferences*, *262*, 11002. https://doi.org/10.1051/matecconf/201926211002

Fenton, G. A., & Vanmarcke, E. H. (1990). Simulation of random fields via local average subdivision. *Journal of Engineering Mechanics*, *116*(8), 1733–1749. Scopus. https://doi.org/10.1061/(ASCE)0733-9399(1990)116:8(1733)

Georgiadis, K. (2010). Undrained bearing capacity of strip footings on slopes. *Journal of Geotechnical and Geoenvironmental Engineering*, *136*(5), 677–685. https://doi.org/10.1061/(ASCE)GT.1943-5606.0000269

Griffiths, D. V., & Fenton, G. A. (2000). Influence of soil strength spatial variability on the stability of an undrained clay slope by finite elements.*Slope stability 2000*, 184–193. https://doi.org/10.1061/40512(289)14

Griffiths, D. V., & Fenton, G. A. (2001). Bearing capacity of spatially random soil: The undrained clay Prandtl problem revisited. *Géotechnique*, *51*(4), 351–359. https://doi.org/10.1680/geot.2001.51.4.351

Hicks, M. A., Nuttall, J. D., & Chen, J. (2014). Influence of heterogeneity on 3D slope reliability and failure consequence. *Computers and Geotechnics*, *61*, 198–208. https://doi.org/10.1016/j.compgeo.2014.05.004

Hicks, M. A., & Samy, K. (2002). Influence of heterogeneity on undrained clay slope stability. *Quarterly Journal of Engineering Geology and Hydrogeology*, *35*(1), 41–49. https://doi.org/10.1144/qjegh.35.1.41

Hicks, M. A., & Spencer, W. A. (2010). Influence of heterogeneity on the reliability and failure of a long 3D slope. *Computers and Geotechnics*, *37*(7), 948–955. https://doi.org/10.1016/j.compgeo.2010.08.001

Huang, J., Lyamin, A. V., Griffiths, D. V., Krabbenhoft, K., & Sloan, S. W. (2013). Quantitative risk assessment of landslide by limit analysis and random fields. *Computers and Geotechnics*, *53*, 60-67.

Li, Y. J., Hicks, M. A., & Nuttall, J. D. (2015). Comparative analyses of slope reliability in 3D. *Engineering Geology*, *196*, 12–23. https://doi.org/10.1016/j.enggeo.2015.06.012

Lodahl, M. R., Brødbæk, K. T., Sørensen, C. S., & Sørensen, J. D. (2012). Reliability-based calibration of partial factors for design of railway embankments. *Proceedings of the 16th Nordic Geotechnical Meeting*, *1*, 381–388.

Luo, N., & Bathurst, R. J. (2017). Reliability bearing capacity analysis of footings on cohesive soil slopes using RFEM. *Computers and Geotechnics*, *89*, 203–212. https://doi.org/10.1016/j.compgeo.2017.04.013

Meyerhof, G. G. (1957). The ultimate bearing capacity of foundations on slopes. *Proc., 4th Int. Conf. on Soil Mechanics and Foundation Engineering*, *1*, 384–386.

Savolainen, L., Mansikkamäki, J., & Kalliainen, A. (2017). 2D loads for stability calculations of railway embankments: 3D FEM comparison between load models and uniformly distributed area loads in stability calculations.*Liikenneviraston julkaisut [1241]*. https://www.doria.fi/handle/10024/147583

van den Eijnden, A. P., & Hicks, M. A. (2017). Efficient subset simulation for evaluating the modes of improbable slope failure. *Computers and Geotechnics*, *88*, 267–280. https://doi.org/10.1016/j.compgeo.2017.03.010

Varkey, D., Hicks, M. A., & Vardon, P. J. (2023). Effect of uncertainties in geometry, inter-layer boundary and shear strength properties on the probabilistic stability of a 3D embankment slope. *Georisk: Assessment and Management of Risk for Engineered Systems and Geohazards*, *17*(2), 262–276. https://doi.org/10.1080/17499518.2022.2101066